JAAS

Journal of Analytical Atomic Spectrometry

Accepted Manuscript

This article can be cited before page numbers have been issued, to do this please use: L. J. Fernández-Menéndez, C. Méndez-López, C. González Gago, J. Pisonero and N. Bordel, *J. Anal. At. Spectrom.*, 2023, DOI: 10.1039/D2JA00343K.

ROYAL SOCIETY OF CHEMISTRY

rsc.li/jaas

Improving Cl determination in cements by molecular LIBS using noble gas-enriched atmospheres and new approaches for interference removal

Luis Javier Fernández-Menéndez, Cristina Méndez-López, Cristina González-Gago, Jorge Pisonero* and Nerea Bordel*.

University of Oviedo, Department of Physics. Federico García Lorca 18, 33007, Oviedo, Asturias, Spain.

Keywords: Laser Induced Breakdown Spectroscopy (LIBS), molecular spectra, chlorine determination, CaCl emission bands, cement.

Abstract

Nowadays, emission from diatomic molecules is frequently used for multiple purposes within Laser-Induced Breakdown Spectroscopy (LIBS). However, these spectrally broad signals are often found interfered by other spectral emissions, which can be detrimental for analytical purposes. In the particular case of chlorine determination in cements via CaCl emission (~593 nm), the spectral interferences are caused by molecular CaO (~590-620 nm) and atomic Na I (~590 nm) emissions. In this work, a methodology to remove both CaO and Na interferences was developed and critically evaluated, overcoming the problematics associated with the absence of a Cl-blank cement sample and the variability of Na concentration in the analyzed samples. Moreover, the generation of the plasma in Ar- and He-enriched atmospheres was also investigated, concluding that the use of Ar is recommended to improve Cl determination since it yields a higher sensitivity while maintaining a lower contribution of the Na interferences. The suitability of the developed protocol was demonstrated through the successful determination of Cl content in real cement samples, with concentrations ranging between 0.23 and 1.5 wt.% of Cl.

View Article Online
DOI: 10.1039/D2JA00343K

1. Introduction

Laser-induced breakdown spectroscopy (LIBS) is a technique based on the generation and spectral analysis of the emission of a laser-induced plasma (LIP), which can be produced on the surface of any kind of material. It is typically applied for analytical purposes, since the spectral information obtained can be used to determine the multi-elemental composition of the material [1–4]. Moreover, LIBS is a cost-effective technique, suitable for analyzing samples in situ and without prior preparation. These characteristics make it very convenient for its implementation as portable and/or remote-controlled (standoff) devices, operating in areas with limited or no human access, such as underwater or even in planetary exploration [3].

The development of LIBS-based methodologies for halogen detection, and especially for chlorine, is increasing. For example, LIBS was recently employed to determine the presence of Cl in the frescoes of Pompeii [5], [6], in liquids [7], and in different salts under simulated Martian conditions as it is an element to be determined in samples of geological interest on Mars [8,9]. In fact, the ChemCam instrument on the Curiosity rover reported the presence of Cl on the Martian surface through CaCl emission [10]. Furthermore, special attention is paid to the determination of Cl in cements [11,12,21–25,13–20] due to possible damaging processes in reinforced concrete. Nevertheless, as an atomic emission-based technique, LIBS has limitations for halogen element determination in terms of sensitivity and limits of detection. Halogens have high ionization/excitation energies, so their resonant emission lines are in the VUV spectral range (<200 nm), requiring specific detection systems operating in vacuum [26]. Since most of the LIBS set-ups are not operated in vacuum, the most straightforward option is to use the less-intense lines corresponding to transitions in the VIS-IR spectral region (600-900 nm), but their weak emission leads to a limited detection sensitivity. In order to overcome this drawback, several alternatives enhancing the VIS-IR signals are commonly employed in LIBS: (a) the generation of the plasma in a He-rich atmosphere that results in the reduction of background emission, improving the atomic IR signal [19–23,27–29]; (b) the use of a second laser pulse acting as a re-excitation source that enhances the atomic signal [11,17,18,23–25]; (c) the indirect determination of the halogen via the study of the emission from diatomic molecules consisting of an alkaline earth and the halogen, whose formation is likely to occur in a LIP. This last method has been extensively studied [5,6,35–39,8–10,30–34]. The use of molecular signals yields a simple experimental configuration while achieving low limits of detection (LODs) and quantification (LOQ). Moreover, this approach is very appropriate for the determination of Cl in cements, given that Ca is a major compound of the material and therefore CaCl bands are present in LIPs spectra. Previous works successfully applied this methodology for Cl determination in concrete [12–15,17].

The generation of the plasma in a noble gas-enriched atmosphere changes fundamental plasma parameters such as the excitation temperatures or the electron densities [40]. As a result, enhancement can be achieved not only for the atomic emission, but also for the molecular emission of the plasma. In this line, alternatives (a) and (c) were successfully combined in cements for Cl determination [14,15,17], where He was used as buffering gas and Cl was detected through molecular CaCl signal. However, the effects of other buffering gases in CaCl signal have not been reported so far. Specifically, Ar is a promising buffer gas candidate since it was already used for atomic [40–42], and also for molecular CaF signal enhancement [43]. Another substantial improvement in the accuracy of Cl determination involves the proper processing of the spectral interferences within the spectral CaCl bands, which are strongly interfered by several emission signals from CaO, Ca and Na.

View Article Online
DOI: 10.1039/D2JA00343K

A common alternative to overcome this problem is to apply polynomial functions to fit the background and then remove it [8,15]. Another innovative solution was recently proposed [13], demonstrating that an statistical method like Partial Least Squares (PLS) is also able to minimize the CaO interferences from the CaCl emission for quantification purposes. In this context, it is necessary to be especially cautious in the procedures of normalization and interference removal in order to obtain a reliable calibration with the highest sensitivity. A detailed Cl quantification protocol was recently evaluated using CaCl emission ($B^2\Sigma \rightarrow X^2\Sigma$ electronic transition, $\Delta v=0$ sequence), showing that spectral interference from CaO could be removed by using a blank sample, and employing variable integration ranges led to an improved sensitivity and a reduced uncertainty [44]. Nevertheless, this procedure is not enough for cement samples due to their high amount of sodium content, as the bright orange doublet which characterizes the Na I emission spectrum (~589 nm), significantly interferes the $B^2\Sigma \rightarrow X^2\Sigma$ $\Delta v=0$ emission of CaCl (~593 nm). In addition, blanks containing suitable amounts of Na are often not available for the analysis of such samples, so further efforts are needed in order to remove this interference. Thus, the purpose of this work is to investigate how the application of Ar and He in the plasma surroundings affects the CaCl signal, and to determine the conditions under which of these gases can enhance CaCl detection. In addition, an improved methodology to properly deal with simultaneous interferences from both Na I and CaO is also developed and evaluated in order to accurately quantify Cl in cement samples notwithstanding their significant sodium content and the lack of suitable blank samples.

2. Experimental

2.1 Sample features

The samples used in this work were manufactured by BAM (*Bundesanstalt für Materialforschung und –prüfung,* Berlin) and by IBAC (Institut für Baustoffforschung der RWTH Aachen Univeristät, Aachen), in the context of an international laboratory comparison for the determination of Cl in cement paste.

Regarding sample preparation [45], water and cement (initial w/c ratio of 0.5, DIN EN 197-1 [46]) were homogenized in a mortar, and different amounts of NaCl were added in order to establish a specific Cl content (see Table 1). Then samples were dried, grounded and pressed into pellets (diameter 35 mm, thickness 4 mm). Samples were divided into two sets: calibration samples and test samples. The calibration samples were based on CEM I with NaCl addition. Test samples were similarly produced, introducing differences in some of the samples in order to study the matrix effects. Specifically, the cement type was varied in samples T05 and T06, and the additive was changed to KCl in sample T07 (Table 1). To test the reproducibility of the methodology, sample T02 and T08 were prepared from the same cement paste powder.

Since no blank sample was included in the provided sample set, 5 g a 98.5 % purity calcium carbonate powder ($CaCO_3$, Sigma Aldrich) were crushed and pelletized under 60 s long hydraulic pressing at 10 tones (Specac, T-40, Atlas Series Evacuable Pellet Dies) to obtain a cylindrical pellet with a diameter of 32 mm and 4 mm thick, from which a clean CaO spectrum could be obtained.

Table 1. Chlorine mass concentrations in the cement samples. The table also lists the type of cement used and the additive employed to provide Cl. Note that the Cl concentration for K01 is the natural content in CEM I cement paste.

View Article Online
DOI: 10.1039/D2JA00343K

Sample	Role	Cement type	Additive	wt.% of Cl
K01	Calibration	CEM I	--	0.06
K02	Calibration	CEM I	NaCl	0.19
K03	Calibration	CEM I	NaCl	0.32
K04	Calibration	CEM I	NaCl	0.46
K05	Calibration	CEM I	NaCl	0.59
K06	Calibration	CEM I	NaCl	0.72
K07	Calibration	CEM I	NaCl	0.85
K08	Calibration	CEM I	NaCl	0.98
K09	Calibration	CEM I	NaCl	1.15
K10	Calibration	CEM I	NaCl	1.43
K11	Calibration	CEM I	NaCl	1.71
K12	Calibration	CEM I	NaCl	1.95
T01	Test	CEM I	NaCl	1.51
T02	Test	CEM I	NaCl	0.50
T03	Test	CEM I	NaCl	1.02
T04	Test	CEM I	NaCl	0.23
T05	Test	CEM II/B-LL	NaCl	0.41
T06	Test	CEM III/A	NaCl	0.87
T07	Test	CEM I	KCl	0.59
T08	Test	CEM I	NaCl	0.50

2.2 LIBS setup

The excitation source employed in this work is a Q-Switched Nd:YAG 1064 nm laser beam (EKSPLA, NL301HT), operated at 5 Hz. An energy of 100 mJ per laser shot was set using an attenuator (LOTIS-TII). The laser beam was then focused on the sample surface by means of an objective (Thorlabs, LMH-5X-1064, 35 mm focal length). To perform a controlled scan of the sample surfaces, a X-Y platform moved by two stepper motors (a commercial PImiCos GmbH VT_80200-2SM and a custom unit manufactured by the University of Oviedo) were used. Light from the plasma was focused through two plano-convex lenses (Thorlabs, LA4904-UV and LA4904-UV), forming its image on the spectrograph entrance slit plane. The spectrographic system was comprised by a Czerny-Turner spectrometer of 500 mm focal length (Andor Technology, Shamrock SR-500i-D1) coupled to an ICCD (Andor Technology, iStar DH734-25F-03). Noble gas-enriched atmospheres were achieved blowing the gases by means of a plastic nozzle of 4 mm diameter. This element was pointing the ablation area from 1 cm above the sample, forming an angle of 50° with respect to the surface. The mass flow controller (MKS Instruments) was set at 1.8 L/min for Ar and He, both supplied by AirLiquid (purity > 99.999 %). This conventional LIBS configuration was already used in previous studies and a scheme can be found in [43].

Each sample spectrum is the result of the in-software accumulation of 20 spectra from consecutive laser shots, all of them acquired using a grating of 1200 lines/mm positioned to collect light wavelengths between 577 and 610 nm. Ten spectra were acquired per sample for statistical purposes, so a total of 200 shots were made in each sample. These laser shots were performed while displacing the sample at 1 mm/s by one of the servomotors, so that each spectrum was obtained from a 4 mm length raster.

View Article Online
DOI: 10.1039/D2JA00343K

3. Results and discussion

3.1 Interference removal methodology.

The first task addressed in this work was the removal of interferences searching the proper way to obtain reliable data. The first task addressed in this work was the removal of interferences searching the proper way to obtain reliable data. To evaluate the validity of the interference elimination procedure for all Cl concentrations, the calibration samples (K01-K12) were measured in air using a delay time of 50 μs and a gate time of 15 μs. This delay time was chosen following the results obtained in a previous work [44] which showed for this delay a good balance between the already low atomic emission intensities of Na and Ca and the still high molecular emission of CaCl in gypsum samples. On the other hand the gate in this study was set for the spectrum of the sample with the highest NaCl content (K12) to have its maximum intensity under the limit of the linear response of the detector (40,000 counts).

In a first data treatment step, removal of the dark current (~4000 counts) was applied to the raw emission spectra, followed by a spectral normalization to the background emission. This implied dividing the signal of each individual spectrum by the average intensity between 577.1 and 577.5 nm, which was representative of background continuum emission. As previously described, the CaO signal interfering the CaCl emission (see Figure 1a) can be spectrally removed by subtracting the corresponding average spectrum of a Cl-free blank sample. Due to the absence of a blank cement sample, $CaCO_3$ was used instead. However, the CaO spectrum obtained from the blank did not properly fit the CaO emission seen in cements. This is shown in Figure 1a, where normalized spectra (after dark current removal and background normalization) from sample K10 and from $CaCO_3$ are plotted. To counter this matrix effect, the $CaCO_3$ average spectrum (blank) was rescaled to fit each sample spectra at 596 nm, which represents the upper limit of the selected CaCl emission. The rescaling factor was between 0.98 and 1.02 in all cases. Figure 1b shows the $CaCO_3$ sample spectrum after rescalation, to properly fit the background CaO emission in the K10 cement spectrum. The removal of CaO interference was therefore enabled by the spectral subtraction of the rescaled blank average spectrum (Figure 1c).

View Article Online
DOI: 10.1039/D2JA00343K

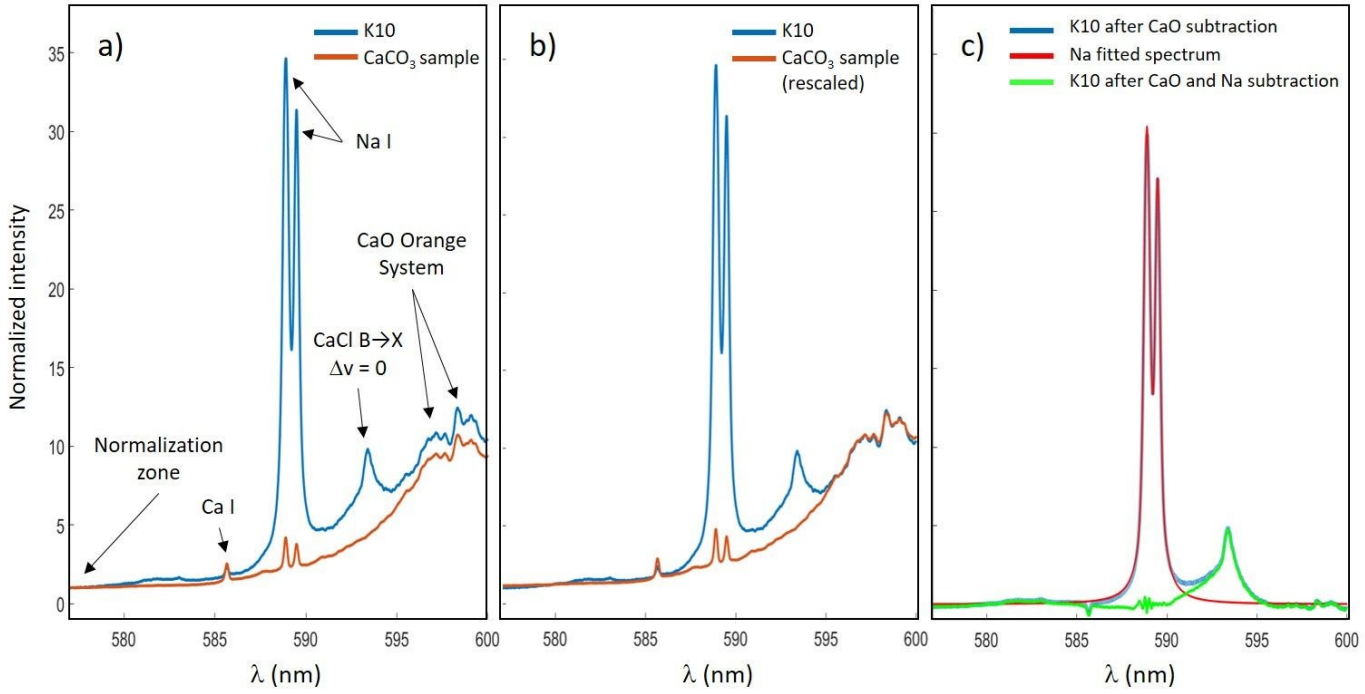

Figure 1. a) Spectral emission from K10 and the $CaCO_3$ sample after dark current removal and background normalization. b) Rescalation of the $CaCO_3$ spectrum. c) In blue, spectrum from K10 after the subtraction of the rescaled $CaCO_3$ sample spectrum, in red the fitted Na emission spectrum and in green the K10 spectrum after interference of CaO and Na removal.

Once the CaO interference was removed, the removal of the Na interference was addressed. For this purpose, the profile of each one of the two Na I emission lines was approximated by a pseudo-Voigt profile (see details of the fitting model in the supplementary material) [47]. The least-squares regression was applied to the data points where the Na lines predominate, which is between 588.28 and 590.21 nm. Note that this regression was done individually for every single spectrum after CaO background removal. Figure 1c shows the consistent fitting of the Na lines, enabling their removal by subtracting the computed profiles. Although in these spectra the residuals of the Na lines could not be completely removed in the range 588-590 nm, the contribution of the Na line wings to the spectra can be properly removed allowing then the extension of the CaCl signal integration range down to 590 nm in its lower limit (Figure 1c).

3.2 Optimization and selection of the buffering gas for CaCl determination

As discussed in the introduction, the generation of the plasma in a noble gas-enriched atmosphere changes the behavior of the plasma emission. Therefore, the possible variations in the temporal evolution of the CaCl emission produced by the blowing gas need to be study in order to select the best acquisition conditions for each atmosphere.

Sample K03 was selected for this optimization, as it contains a low Cl concentration, but enough for the CaCl emission to be clearly visible. Table 2 lists the acquisition conditions at which the spectra were measured in each one of the 3 environments: air, Ar, and He. Note that the gate times were set in order to ensure that Na I emission lines (588.99 nm and 589.59 nm, respectively) remained within the linear response range of the detector.

Table 2. Acquisition conditions evaluated for delay time optimization. Delay was varied from 20 to 60 μs for air and He measurements , while from 30 to 70 μs for Ar ones since the emission decay is slower for the latter [40,43].

Delay (μs)	Gate (μs)
20	3
30	5
40	10
50	15
60	15
70	15

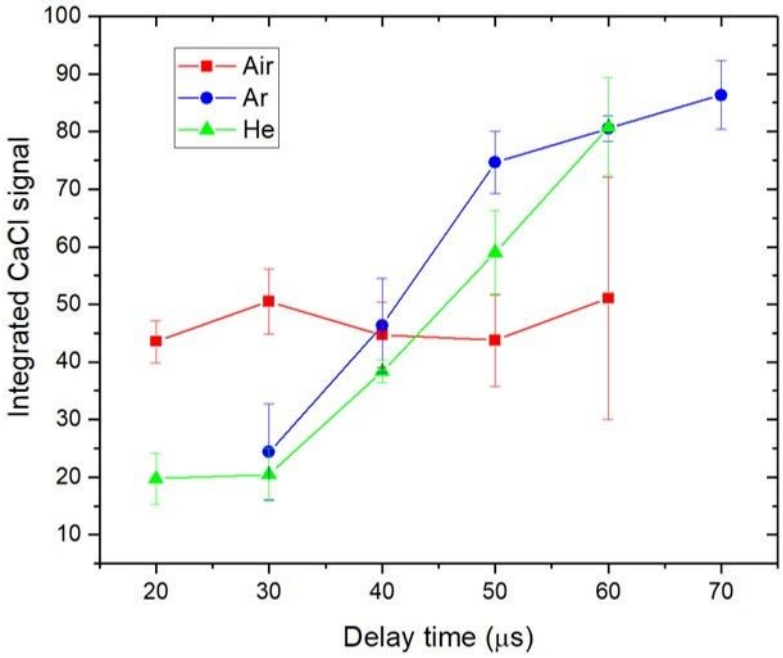

Figure 2. Integrated CaCl signal from sample K03 in terms of the delay time for each medium.

All the acquired spectra were processed as reported in section 3.1, and the integrated signals for each condition are shown in Figure 2. Note that the integration range was fixed from 591.5 to 594.65 nm. In case of air environment, the integrated signal remains almost constant (~45). Conversely, when blowing either Ar or He, the CaCl signal experiences a significant increase with the delay time. Particularly, acquisition delays ≥ 50 μs showed higher CaCl intensities for Ar and He experiments. Nevertheless, it is observed that experiments in He provided Na emission lines with higher intensities than those obtained in Ar (Figure 3), extending its contribution to higher wavelengths. Although this contribution can be significantly removed by subtracting the fitted Na, it is convenient to firstly minimize its influence by purely experimental procedure before resorting to data treatment, especially for samples contain high Cl concentrations (~1%). Therefore, the use of the Ar atmosphere has been considered as the most favorable environment for subsequent calibration and quantification because of the lower Na emission intensities. It should be noted that, before normalization, all the intensities of the assessed emissions (Na, CaO, CaCl, background, …) showed higher intensities when blowing Ar and lower for He, comparing to those in air. However, the reported behavior of the CaCl signal can be achieved when normalization to the spectral background is applied, since the assessed CaCl signal is the one relative to its background emission [44].

View Article Online
DOI: 10.1039/D2JA00343K

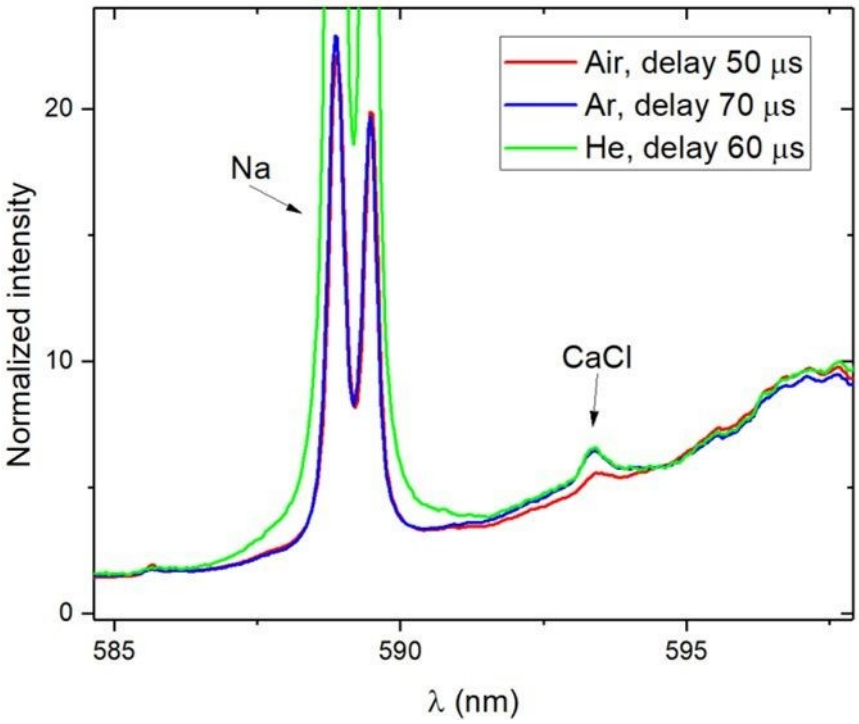

Figure 3. Average spectra taken from sample K03, corresponding to the conditions with higher CaCl emission for each medium.

3.3 Calibration performance

The calibration samples shown in Table 1 were utilized to obtain calibration curves not only under Ar environment but also in air, as to explicitly evaluate the analytical features improvement provided by Ar blowing. Note that both series were acquired at their respective optimal conditions, i.e. delay times of 50 and 70 μs for air and Ar, respectively. After the acquisition and processing, interference-free spectra are obtained (Figure 4) and they can be straightforwardly integrated to get the net CaCl signal. Figure 4 shows a clear enhancement of CaCl emission when Ar is used, indicating an effective improvement in the sensitivity compared to air. It is observed that the detected CaCl emission extends over different spectral ranges according to the Cl concentration. For instance, in Figure 4 it is noticed that the CaCl bands from the sample K12 (1.95 wt.% of Cl) cover a spectral window of 6 nm, while that of K01 (0.06 wt.% of Cl) is restricted to a narrow 1 nm range. If both signals were to be integrated between 590 and 596 nm, the value for K01 would be significantly influenced by noise fluctuations rather than CaCl signal, increasing its uncertainty. Therefore, the choice of an optimum spectral integration range is crucial to obtain a reliable calibration. As performed in a previous work [44], a variable integration range was therefore applied, restricting each sample range to the spectral region in which the CaCl emission is above the 8 % of its maximum intensity, measured at 593.50 nm. Integrating the emission outside this boundary hardly contributes to the net intensity value yet might increase its uncertainty, especially for samples with lower Cl content.

View Article Online
DOI: 10.1039/D2JA00343K

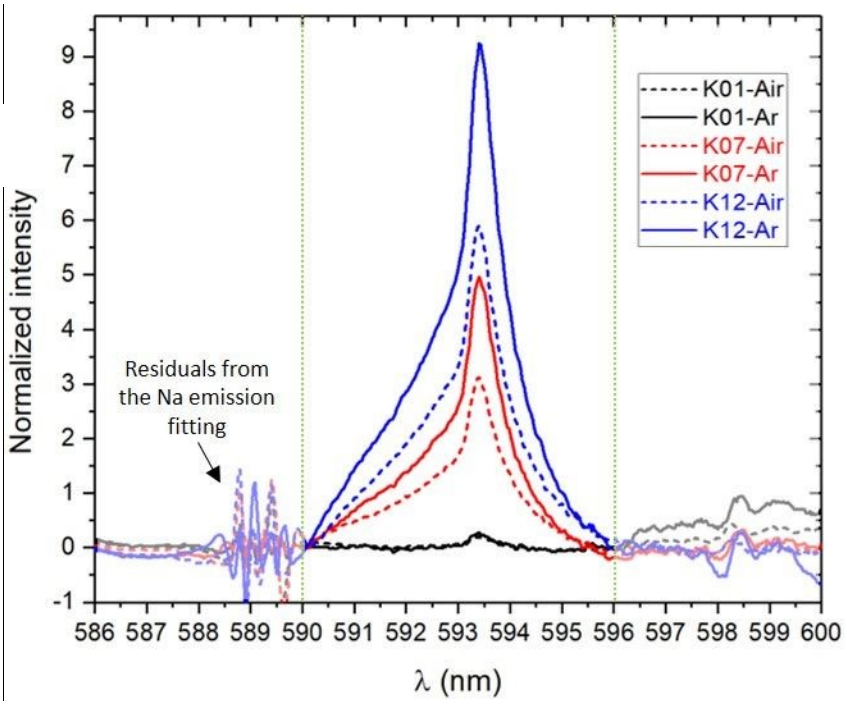

Figure 4. Interference-free spectra from samples K01, K07 and K12. Solid lines represent the spectra taken in Ar and dashed lines that taken in air. Note that the green dotted vertical lines indicate the widest integration range.

Linear calibration curves were obtained for air and Ar (Figure 5), relating the CaCl signal to the Cl concentration, and a variance-weighted least squares linear fitting was performed [48]. The uncertainty of each data point is the stardard deviation (σ) of the 10 net CaCl signals obtained per sample. The resulting equations are shown in the insets of Figure 5. In absence of a certified blank of the analyzed material, the background estimation was obtained from the lower Cl-content sample spectra, K01, by using a spectral region adjacent to that of the integrated CaCl signal (593.14-594.14 nm for air and 592.33-594.30 nm for Ar) [49]. Specifically, the integration range used for background integration in air was 594.14-595.14 nm, and that for Ar was 594.30-595.97 nm, i.e. displacing the CaCl integration windows employed for K01 to the spectral background position (black series, Figure 4). It should be noted that for higher concentrations a proper background cannot be defined, since both below 590 nm and above 596 nm, the signal is highly interfered by Na and CaO emissions, respectively. The standard deviation of the 10 integrated background values (σ_B) was used to calculate the LODs (inset of Figure 5), using the $3\sigma_B$ criteria.

View Article Online
DOI: 10.1039/D2JA00343K

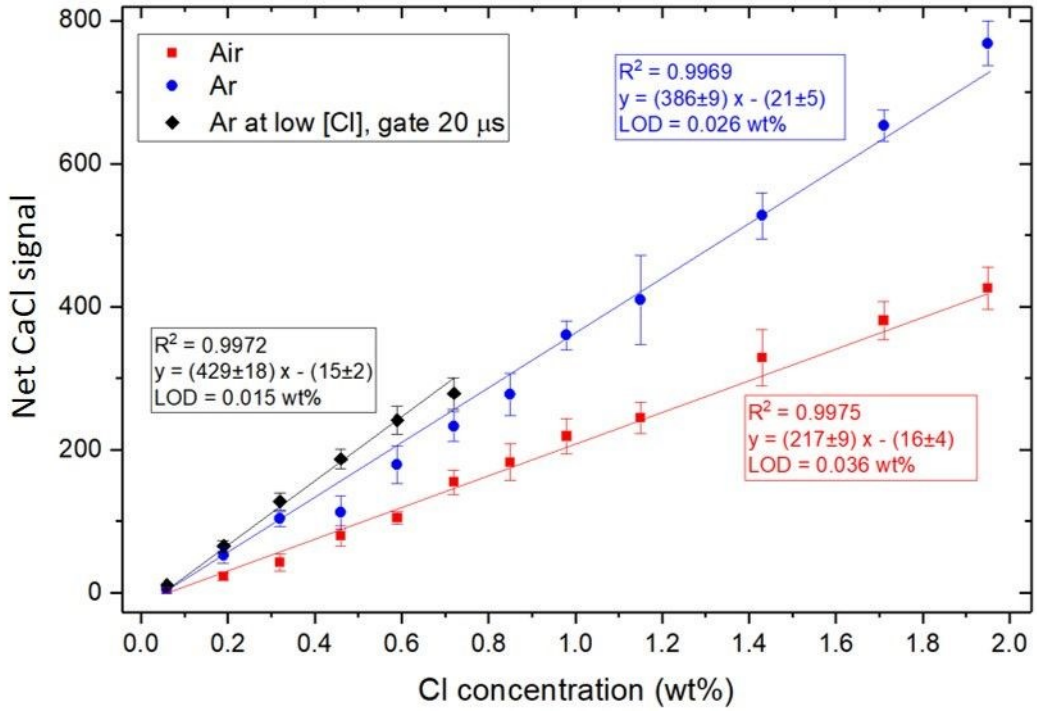

Figure 5. Calibration of Cl content for the K01-12 samples through CaCl signal integration, their linear regressions parameters and their corresponding LODs. The red series corresponds to the air and the blue series to the Ar measurements. In black, the low Cl-content calibration (samples K01-06) performed in Ar with a longer gate time of 20 µs.

As shown in Figure 5, the improvement achieved by blowing Ar in the vicinity of the plasma is clear, reducing the LOD from 0.036 to 0.026 wt.% of Cl. However, further improvement in the LOD was achieved by redoing the calibration in Ar only for low Cl concentration samples (K01-K06, Figure 5) employing a longer gate of 20 µs. In general, the gate time of the acquisition used for calibration is upper limited by the spectral intensity of the sample with the highest concentration (K12), since it is set to avoid exceeding the linear range of the detector, as discussed above. By employing a longer gate of 20 µs, a slight increase in the CaCl signal is achieved as well as a reduction of the spectral background noise (σ_B), resulting in improved LOD, reducing it almost by half (0.015 wt.% of Cl).

3.4 Quantification of Cl with Ar flow

To verify that the methods described in the previous sections are effective, the Cl content of the test samples was quantified. Due to its good performance, Ar was chosen as blowing gas. Specifically, the test samples were measured under the optimum acquisition conditions of 70 µs delay and 15 µs gate, analogous to the calibration of K01-K12. The determination of the Cl concentration was performed by calculating the predicted concentration value ($\hat{x}$) using the fitting line equation (blue and black series in Figure 6). Uncertainties for the test samples concentrations ($\sigma_{\hat{x}}$) were obtained through the partial derivative error propagation procedure applied to the $\hat{x}$ expresion [48]. Both the estimated concentration ($\hat{x}$) for each sample and its uncertainty ($1\sigma_{\hat{x}}$) are plotted (see Figure 6).

View Article Online
DOI: 10.1039/D2JA00343K

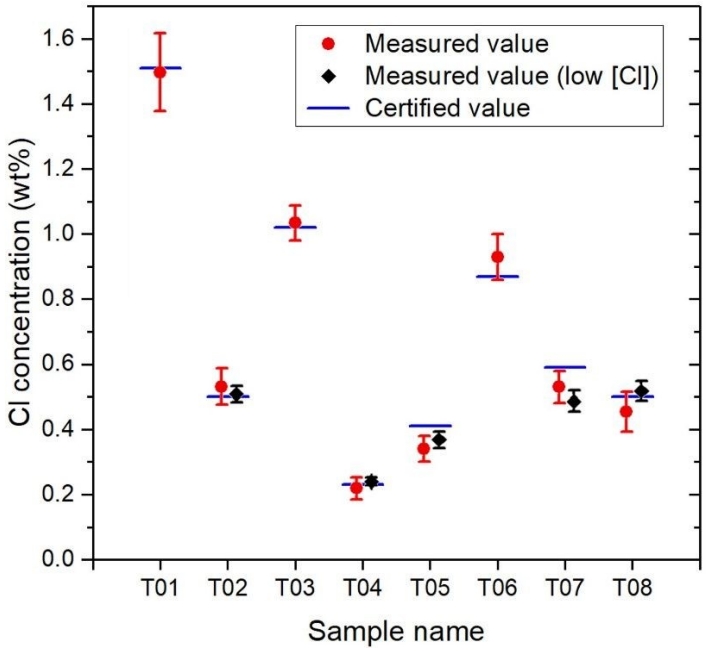

Figure 6. Estimated Cl concentration for the whole set of test samples and their reference values. In red, results for the samples measured at 70 μs delay and 15 μs gate. In black, results for the low Cl content samples, measured at 70 μs delay and 20 μs gate.

As can be seen in Figure 6 (red series), the estimated Cl concentrations for T01, T02, T03, T04, T06 and T08 samples are in agreement with the reference value of Cl concentration. However, the results for T05 sample (sample with a different cement type) and T07 sample (sample where KCl was added instead of NaCl) are slightly underestimated. Moreover, it is noticed that the analysis of samples containing less than 0.6 wt.% of Cl (T02, T04, T05, T07, T08) showed lower precision (uncertainties around 12 %, and relative deviation from the reference value of 5 %). Nevertheless, the use of the calibration based on low Cl concentrated samples (black series in Figure 6) resulted in improved precision and accuracy (uncertainties were reduced from 12 to 6% on average, and their relative errors from 5 % to 3 %) except for sample T07. In this last case the presence of K might be displacing Ca in the formation of halide molecules, resulting in less Cl available to form CaCl. This effect would lead to a decrease in CaCl emission, consistent with the underestimation of the Cl content for sample T07.

4. Conclusions

A detailed protocol has been described and applied to determine Cl in cement samples by means of CaCl molecular emission from a laser-induced plasma. In particular, a discussion about dealing with high amounts of Na and lack of blank samples has been presented, including a method to spectrally remove the CaO and Na interferences. Regarding the CaO interference, it was found that spectral normalization to the background followed by a rescaling of a spectrum taken from a $CaCO_3$ sample can be used to remove this interference in absence of a blank cement sample. Furthermore, a pseudo-Voigt function fit was firstly used to successfully remove the interference from the Na I emission lines. Both Ar and He blowing were evaluated as possible sources of improvement for Cl determination through molecular emission, finding that both provide a remarkable enhancement of the CaCl signal with respect to the results in air. However, He also enhances the Na interference, so its use was discarded and only Ar was employed for quantification purposes. Spectral integration of CaCl with variable ranges was applied on the analyzed samples, showing that this method is also

suitable for the determination of Cl in cement matrix. It is worth mentioning that all the calibrations performed yielded linear behaviors, offering linear ranges of up to 2 wt.% of Cl, and achieving a LOD of 0.015 wt.% of Cl. The developed methodology was supported by the results obtained from the Cl quantification in the test samples (not considered in the calibration curves), where for all matrix-matched test samples consistent Cl concentration values to those of the validation results were determined. In the case of non matrix matched samples, a slight underestimation of the Cl content was found in the sample containing KCl instead of NaCl as the source of Cl.

Acknowledgements

The financial support from the Spanish Government through the project MCI-21-PID2020-113951GB-I00 / AEI / 10.13039/501100011033 and the predoctoral grant MINECO BES-2017-080768 is gratefully acknowledged. Financial support from the Government of the Principality of Asturias through the predoctoral grant PA-21-PF-BP20-059 is also recognized.

The authors would like to thank Gerd Wilsch and Tobias Völker from BAM (*Bundesanstalt für Materialforschung und –prüfung,* Berlin), for providing the sample material as part of an international interlaboratory comparison.

Bibliography

1. Cremers DA, Radziemski LJ. Handbook of Laser-induced Breakdown Spectroscopy. Handbook of Laser-induced Breakdown Spectroscopy. John Wiley and Sons; 2006. 1–283 p.

2. Hahn DW, Omenetto N. Laser-induced breakdown spectroscopy (LIBS), part I: Review of basic diagnostics and plasmaparticle interactions: Still-challenging issues within the analytical plasma community. Appl Spectrosc. 2010;64(12).

3. Hahn DW, Omenetto N. Laser-induced breakdown spectroscopy (LIBS), part II: Review of instrumental and methodological approaches to material analysis and applications to different fields. Appl Spectrosc [Internet]. 2012 Apr 1 [cited 2019 Jan 6];66(4):347–419. Available from: http://journals.sagepub.com/doi/10.1366/11-06574

4. Russo RE, Mao XL, Yoo JH, Gonzalez JJ. Laser Ablation. Laser-Induced Break Spectrosc [Internet]. 2007 Jan 1 [cited 2019 Jan 3];49–82. Available from: https://www.sciencedirect.com/science/article/pii/B9780444517340500065

5. Pérez-Diez S, Fernández-Menéndez LJ, Morillas H, Martellone A, De Nigris B, Osanna M, et al. Elucidation of the Chemical Role of the Pyroclastic Materials on the State of Conservation of Mural Paintings from Pompeii. Angew Chemie - Int Ed [Internet]. 2021 Dec 3 [cited 2021 Jan 7];60(6):3028–36. Available from: https://onlinelibrary.wiley.com/doi/10.1002/anie.202010497

6. Pérez-Diez S, Fernández-Menéndez LJ, Veneranda M, Morillas H, Prieto-Taboada N, Fdez-Ortiz de Vallejuelo S, et al. Chemometrics and elemental mapping by portable LIBS to identify the impact of volcanogenic and non-volcanogenic degradation sources on the mural paintings of Pompeii. Anal Chim Acta. 2021 Jul 11;1168:338565.

7. Tang Z, Hao Z, Zhou R, Li Q, Liu K, Zhang W, et al. Sensitive analysis of fluorine and chlorine elements in water solution using laser-induced breakdown spectroscopy assisted with molecular synthesis. Talanta. 2021 Mar 1;224:121784.

8. Vogt DS, Rammelkamp K, Schröder S, Hübers HW. Molecular emission in laser-induced breakdown spectroscopy: An investigation of its suitability for chlorine quantification on Mars. Icarus. 2018 Mar 1;302:470–82.

9. Vogt DS, Schröder S, Rammelkamp K, Hansen PB, Kubitza S, Hübers H-W. CaCl and CaF emission in LIBS under simulated Martian conditions. Icarus [Internet]. 2020 Jan 1 [cited 2019 Nov 7];335:113393. Available from: https://www.sciencedirect.com/science/article/pii/S0019103519301563

10. Forni O, Gaft M, Toplis MJ, Clegg SM, Maurice S, Wiens RC, et al. First detection of fluorine on Mars: Implications for Gale Crater's geochemistry. Geophys Res Lett [Internet]. 2015 Feb 28 [cited 2019 Oct 18];42(4):1020–8. Available from: http://doi.wiley.com/10.1002/2014GL062742

11. Zhang Z, Wu J, Hang Y, Zhou Y, Tang Z, Shi M, et al. Quantitative analysis of chlorine in cement pastes based on collinear dual-pulse laser-induced breakdown spectroscopy. Spectrochim Acta - Part B At Spectrosc. 2022 May 1;191:106392.

12. Wakil MA, Alwahabi ZT. Microwave-Assisted laser induced breakdown molecular spectroscopy: Quantitative chlorine detection. J Anal At Spectrom. 2019 Sep 1;34(9):1892–9.

13. Zhang W, Zhou R, Yang P, Liu K, Yan J, Gao P, et al. Determination of chlorine with radical emission using laser-induced breakdown spectroscopy coupled with partial least square regression. Talanta. 2019 Jun 1;198:93–6.

14. Dietz T, Klose J, Kohns P, Ankerhold G. Quantitative determination of chlorides by molecular LIBS. Spectrochim Acta - Part B At Spectrosc. 2019 Feb 1;152:59–67.

15. Dietz T, Gottlieb C, Kohns P, Ankerhold G. Comparison of atomic and molecular emission in LIBS for the quantification of harmful species in cement-based materials. Spectrochim Acta - Part B At Spectrosc. 2019 Nov 1;161:105707.

16. Millar S, Gottlieb C, Günther T, Sankat N, Wilsch G, Kruschwitz S. Chlorine determination in cement-bound materials with Laser-induced Breakdown Spectroscopy (LIBS) – A review and validation. Spectrochim Acta - Part B At Spectrosc. 2018 Sep 1;147:1–8.

17. Omenetto N, Jones WB, Smith BW, Guenther T, Ewusi-Annan E, Florida U of. Feasibility of atomic and molecular laser induced breakdown spectroscopy (LIBS) to in-situ determination of chlorine in concrete : final report. [Internet]. 2016 Oct [cited 2020 Jan 21]. Available from: https://rosap.ntl.bts.gov/view/dot/31477

18. Labutin TA, Popov AM, Raikov SN, Zaytsev SM, Labutina NA, Zorov NB. Determination of chlorine in concrete by laser-induced breakdown spectroscopy in air. J Appl Spectrosc [Internet]. 2013 [cited 2022 Jan 27];80(3):315–8. Available from: https://link.springer.com/content/pdf/10.1007/s10812-013-9766-8.pdf

19. Weritz F, Schaurich D, Wilsch G. Detector comparison for sulfur and chlorine detection with laser induced breakdown spectroscopy in the near-infrared-region. Spectrochim Acta - Part B At Spectrosc. 2007 Dec 1;62(12):1504–11.

20. Wilsch G, Weritz F, Schaurich D, Wiggenhauser H. Determination of chloride content in concrete structures with laser-induced breakdown spectroscopy. In: Construction and Building Materials. Elsevier; 2005. p. 724–30.

21. Gehlen CD, Wiens E, Noll R, Wilsch G, Reichling K. Chlorine detection in cement with laser-

induced breakdown spectroscopy in the infrared and ultraviolet spectral range. Spectrochim Acta - Part B At Spectrosc. 2009 Oct 1;64(10):1135–40.

22. Molkenthin A. Laser-induzierte Breakdown Spektroskopie (LIBS) zur hochauflösenden Analyse der Ionenverteilung in zementgebundenen Feststoffen [Internet]. 2009 [cited 2022 Jan 27]. Available from: www.bam.de

23. Sugiyama K, Fujii T, Matsumura T, Shiogama Y, Yamaguchi M, Nemoto K. Detection of chlorine with concentration of 018 kg/m^3 in concrete by laser-induced breakdown spectroscopy. Appl Opt [Internet]. 2010 [cited 2022 Jan 27];49(13):C181. Available from: https://www.osapublishing.org/abstract.cfm?uri=ao-49-13-c181

24. Gondal MA, Dastageer MA, Maslehuddin M, Alnehmi AJ, Al-Amoudi OSB. Detection of chloride in reinforced concrete using a dual pulsedlaser-inducedbreakdownspectrometersystem: Comparative study of the atomic transition lines of Cl I at 594.85 and 837.59 nm. Appl Opt. 2011 Jul 10;50(20):3488–96.

25. Labutin TA, Popov AM, Zaytsev SM, Zorov NB, Belkov M V., Kiris V V., et al. Determination of chlorine, sulfur and carbon in reinforced concrete structures by double-pulse laser-induced breakdown spectroscopy. Spectrochim Acta - Part B At Spectrosc. 2014 Sep 1;99:94–100.

26. Anderson DE, Ehlmann BL, Forni O, Clegg SM, Cousin A, Thomas NH, et al. [1] D. E. Anderson et al., "Characterization of LIBS emission lines for the identification of chlorides, carbonates, and sulfates in salt/basalt mixtures for the application to MSL ChemCam data," J. Geophys. Res. Planets, vol. 122, no. 4, pp. 744–770, Apr. J Geophys Res Planets [Internet]. 2017 Apr [cited 2019 Jan 7];122(4):744–70. Available from: http://doi.wiley.com/10.1002/2016JE005164

27. Tran M, Sun Q, Smith BW, Winefordner JD. Determination of F, Cl, and Br in solid organic compounds by laser-induced plasma spectroscopy. Appl Spectrosc [Internet]. 2001 Jun 1 [cited 2019 May 8];55(6):739–44. Available from: https://www.osapublishing.org/as/abstract.cfm?uri=as-55-6-739

28. Cremers DA, Radziemski LJ. Detection of Chlorine and Fluorine in Air by Laser-Induced Breakdown Spectrometry. Anal Chem [Internet]. 1983 Jul [cited 2019 May 9];55(8):1252–6. Available from: http://pubs.acs.org/doi/abs/10.1021/ac00259a017

29. St-Onge L, Kwong E, Sabsabi M, Vadas EB. Quantitative analysis of pharmaceutical products by laser-induced breakdown spectroscopy. Spectrochim Acta - Part B At Spectrosc [Internet]. 2002 Jul 31 [cited 2019 May 8];57(7):1131–40. Available from: https://www.sciencedirect.com/science/article/pii/S0584854702000629

30. Gaft M, Nagli L, Eliezer N, Groisman Y, Forni O. Elemental analysis of halogens using molecular emission by laser-induced breakdown spectroscopy in air. Spectrochim Acta - Part B At Spectrosc. 2014;98(June):39–47.

31. Gaft M, Nagli L, Raichlin Y, Pelascini F, Panzer G, Ros VM. Laser-induced breakdown spectroscopy of Br and I molecules with alkali-earth elements. Spectrochim Acta - Part B At Spectrosc. 2019 Jul 1;157:47–52.

32. Gaft M, Nagli L, Gornushkin I, Raichlin Y. Review on recent advances in analytical applications of molecular emission and modelling. Vol. 173, Spectrochimica Acta - Part B Atomic Spectroscopy. Elsevier B.V.; 2020. p. 105989.

33. Alvarez-Llamas C, Pisonero J, Bordel N. A novel approach for quantitative LIBS fluorine

analysis using CaF emission in calcium-free samples. J Anal At Spectrom [Internet]. 2017 [cited 2019 Jan 6];32(1):162–6. Available from: http://xlink.rsc.org/?DOI=C6JA00386A

34. Alvarez-Llamas C, Pisonero J, Bordel N. Quantification of fluorine traces in solid samples using CaF molecular emission bands in atmospheric air LIBS. Spectrochim Acta - Part B At Spectrosc [Internet]. 2016 Sep [cited 2019 Jan 6];123:157–62. Available from: https://linkinghub.elsevier.com/retrieve/pii/S0584854716301343

35. Álvarez C, Pisonero J, Bordel N. Quantification of fluorite mass-content in powdered ores using a Laser-Induced Breakdown Spectroscopy method based on the detection of minor elements and CaF molecular bands. Spectrochim Acta - Part B At Spectrosc. 2014 Oct 1;100:123–8.

36. Resano M, Aramendía M, Nakadi F V., García-Ruiz E, Alvarez-Llamas C, Bordel N, et al. Breaking the boundaries in spectrometry. Molecular analysis with atomic spectrometric techniques [Internet]. Vol. 129, TrAC - Trends in Analytical Chemistry. 2020 [cited 2020 Dec 28]. Available from: https://reader.elsevier.com/reader/sd/pii/S0165993620301849?token=0EA8060BF6A114E0A366BC96660AC124E9F372E6391FBB1D3FC312ED9F01E3FB43EC0F8B9040A969AC351B6BCF39D072

37. Fernández-Menéndez LJ, Méndez-López C, Alvarez-Llamas C, González-Gago C, Pisonero J, Bordel N. Spatio-temporal distribution of atomic and molecular excited species in Laser-Induced Breakdown Spectroscopy: Potential implications on the determination of halogens. Spectrochim Acta - Part B At Spectrosc. 2020 Jun 1;168.

38. Méndez-López C, Álvarez-García R, Alvarez-Llamas C, Fernández-Menéndez LJ, González-Gago C, Pisonero J, et al. Laser induced plasmas at different nebulization conditions: Spatio-temporal distribution of emission signals and excitation temperatures. Spectrochim Acta - Part B At Spectrosc. 2020 Aug 1;170.

39. Vogt DS, Schröder S, Frohmann S, Hansen PB, Seel F, Gensch M, et al. Spatiotemporal characterization of the laser-induced plasma plume in simulated Martian conditions. Spectrochim Acta - Part B At Spectrosc. 2022 Jan 1;187.

40. Aguilera JA, Aragón C. A comparison of the temperatures and electron densities of laser-produced plasmas obtained in air, argon, and helium at atmospheric pressure. Vol. 69, Applied Physics A: Materials Science and Processing. Springer Verlag; 1999. p. S475–8.

41. Rajavelu H, Vasa NJ, Seshadri S. LIBS technique combined with blow gas and vacuum suction to remove particle cloud and enhance emission intensity during characterization of powder samples. Spectrochim Acta - Part B At Spectrosc. 2021 Jul 1;181:106215.

42. Zhang D, Ma X, Wang S, Zhu X. Influence of ambient gas on laser-induced breakdown spectroscopy of uranium metal. Plasma Sci Technol. 2015;17(11):971–4.

43. Bordel N, Fernández-Menéndez LJ, Méndez-López C, González-Gago C, Pisonero J. Halides formation dynamics in nanosecond and femtosecond laser-induced breakdown spectroscopy. Plasma Phys Control Fusion. 2022 May 1;64(5):054010.

44. Fernández-Menéndez LJ, Méndez-López C, Abad C, Fandiño J, González-Gago C, Pisonero J, et al. A critical evaluation of the chlorine quantification method based on molecular emission detection in LIBS. Spectrochim Acta Part B At Spectrosc. 2022 Apr;190:106390.

45. Völker T, Wilsch G. Private communication. 2022.

46. DIN EN 197-1:2011-11 Cement - Part 1: Composition, specificati... [Internet]. [cited 2022 Jan 31]. Available from: https://tienda.aenor.com/norma-din-en-197-1-2011-11-140246044

47. Schmid M, Steinrück HP, Gottfried JM. A new asymmetric Pseudo-Voigt function for more efficient fitting of XPS lines. Surf Interface Anal. 2014;46(8):505–11.

48. Bevington PR, Robinson DK. Data reduction and error analysis for the physical sciences. McGraw-Hill; 1992. 328 p.

49. McNaught A, Wilkinson A, … SP-C, 2004 undefined. "The Gold Book" is now Available in Spanish. degruyter.com [Internet]. [cited 2022 Feb 3]; Available from: https://www.degruyter.com/document/doi/10.1515/ci.2004.26.2.23/html